

Effect of a Polymerizable Cosurfactant on the Microstructure and Drug-Release Properties of Nanoparticles Synthesized through Emulsion Polymerization

Sumit Bhawal,¹ L. Harivardhan Reddy,² R. S. R. Murthy,² Surekha Devi¹

¹Department of Chemistry, Faculty of Science, M. S. University of Baroda, Vadodara 390002, Gujarat, India

²Pharmacy Department, Faculty of Technology and Engineering, Kalabhavan, M. S. University of Baroda, Vadodara 390001, Gujarat, India

Received 25 March 2003; accepted 26 August 2003

ABSTRACT: The emulsion copolymerization of a partially water-soluble monomer, methyl methacrylate (MMA), and a water-soluble polymerizable cosurfactant, hydroxyethyl methacrylate (HEMA), was investigated. The microstructure of the copolymer varied as the HEMA concentration increased. The copolymer microstructure influenced drug entrapment and was studied with respect to the variation in the MMA/HEMA ratio, the crosslinker concentration, and

the method of nanoparticle separation from the dispersion. The subsequent release of a lipophilic drug, carbamazepine, from nanoparticles was studied at three different copolymer compositions. © 2004 Wiley Periodicals, Inc. *J Appl Polym Sci* 92: 402–409, 2004

Key words: emulsion polymerization; nanoparticles; drug release

INTRODUCTION

One of the primary objectives of the design of novel drug-delivery systems is the controlled delivery of a pharmacological agent to its site of action at a therapeutically optimal rate and dose regime.¹ This can not only improve the efficacy of the drug but also reduce the possibility of unwanted toxic side effects of the drug and improve the therapeutic index.² Among the most promising systems for achieving this goal are colloidal drug-delivery systems, which include liposomes, niosomes, nanoparticles, and microemulsions.³ In recent years, polymeric nanoparticles have gained much importance because of their biodegradability, stability due to their rigid structure, and ease of drug encapsulation.

One successful method of preparing polymeric nanoparticles is the compartmentalization of the reaction system.⁴ This can be achieved through an emulsion polymerization of a suitable monomer–surfactant system. This technique offers a system with a lower particle size and good control over its size distribution. Many monomer systems belonging to the class of

acrylic acid esters, such as methyl methacrylate (MMA), alkyl cyanoacrylates, 2-hydroxyethyl methacrylate (HEMA), and methacrylic acid, have been investigated.^{5–8}

Poly(methyl methacrylate) (PMMA) nanoparticles have been reported to show slow biodegradability.⁶ The biodegradability can be improved through the copolymerization of MMA with a monomer such as HEMA that forms a more biodegradable polymer. Recently, Sivakumar and Rao⁹ carried out the polymerization of MMA and HEMA to produce core–shell microspheres, and they further investigated the release of ibuprofen from these microspheres. They showed improved drug release from poly(MMA-co-HEMA) core–shell microspheres in comparison with PMMA microspheres. In this study, we attempted to synthesize nanoparticles through the emulsion copolymerization of MMA and HEMA. Also, we investigated, in some detail, the factors controlling the copolymer microstructure and its effect on the entrapment and release of the lipophilic drug carbamazepine.

EXPERIMENTAL

Carbamazepine (99.8% pure) was obtained as gift sample from Alembic Chemicals, Ltd. (Baroda, India). MMA (BDH, Poole, England), ethylene glycol dimethacrylate (EGDMA; Merck, Schuchardt, Germany), and HEMA (Fluka, Buchs, Switzerland) were purified by vacuum distillation under reduced pres-

Correspondence to: S. Devi (surekha_devi@yahoo.com).

Contract grant sponsor: Council for Scientific and Industrial Research (CSIR) (New Delhi, India).

Contract grant sponsor: University Grants Commission (UGC) (New Delhi, India).

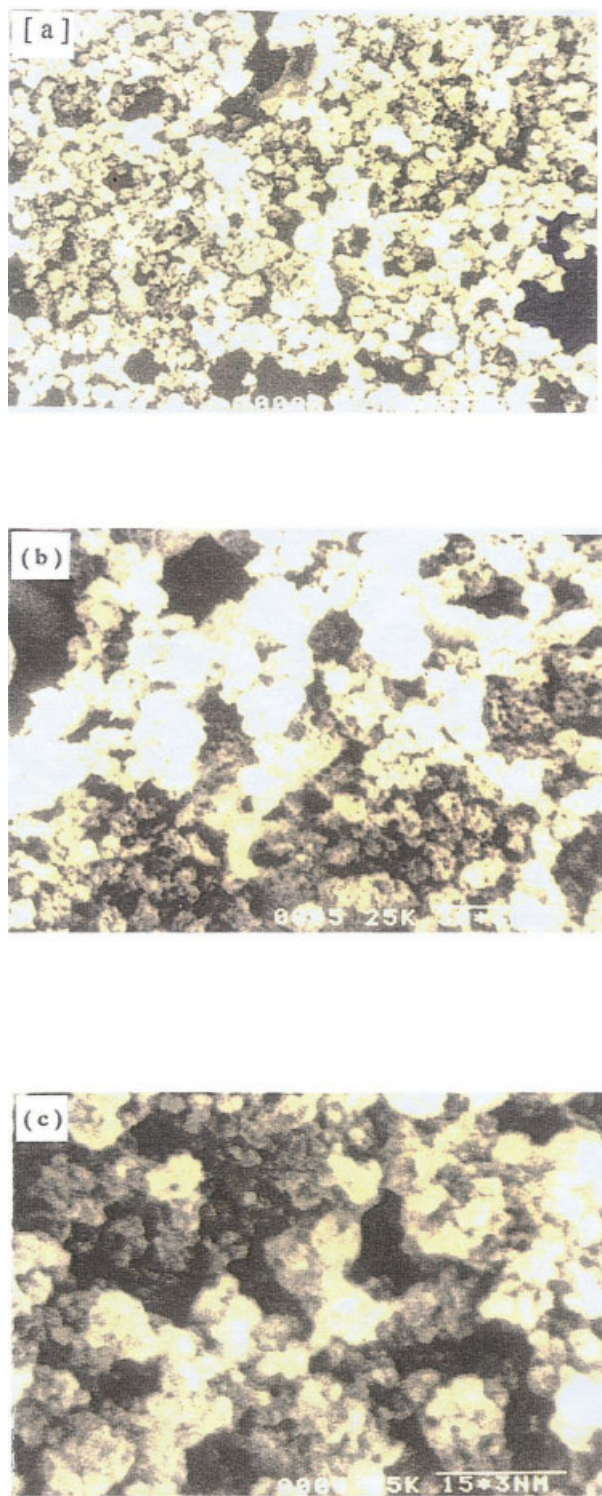


Figure 1 SEM images showing the effect of the monomer composition on the copolymer microstructure at 25,000 \times magnification: (a) 90/10, (b) 80/20, and (c) 70/30 MMA/HEMA.

sure and stored at 4 $^{\circ}$ C until further use. L-Ascorbic acid (Loba, Mumbai, India) and 30% (w/v) H₂O₂ (Merck) were used as a redox initiator system. Sodium lauryl sulfate (SLS; SD Fine Chemicals, Baroda, India)

was used as received. Doubly distilled water was used throughout the experiments.

Emulsion copolymerization

Poly(MMA-co-HEMA) was synthesized by a batch process in an emulsion containing 10% monomer (w/w), 2% SLS, and 88% water. This ternary emulsion was charged in a five-necked reaction kettle equipped with a mechanical stirrer, a water condenser, a thermometer, and a nitrogen inlet. The emulsion polymerization was initiated with a 1/1 (mol/mol) H₂O₂/ascorbic acid redox initiator at 40 $^{\circ}$ C. The polymerization was continued for 4 h for complete conversion. The lipophilic drug carbamazepine was dissolved in the monomer before emulsification. The amount of drug dissolved was 5% with respect to the monomer. After the polymerization, the latex was freed from the surfactant through freezing and thawing below and above the kraft temperature, which was 16 $^{\circ}$ C for SLS. The latex was then freeze-dried and yielded dry nanoparticles.

Characterization

IR spectrum

The IR spectrum of the purified copolymer was recorded on a PerkinElmer 16 PC IR spectrophotometer (Boston, MA) with 1-cm-diameter KBR pellets.

Ultraviolet (UV) spectrum

The UV spectra of the purified copolymer, drug, and drug-containing polymer were recorded on a U 2000 spectrophotometer (Hitachi, Japan) in ethanol.

Particle size analysis

A Malvern 4700 photon correlation spectrophotometer (UK) equipped with a vertically polarized argon-ion laser source operating at 488 nm was used to measure the particle size of the polymerized emulsion latices in a dynamic mode. The scattering intensities from the sample were measured at 90 $^{\circ}$ with the help of a photomultiplier tube. The intensity correlation data were analyzed by the method of cumulants to provide the average decay rate [$\langle \Gamma^2 \rangle = q^2 D$, where $\mathbf{q} = (4\pi n/\lambda)\sin \theta/2$ is the scattering vector, n is the index of refraction, and D is the diffusion coefficient] and the variance ($\nu = \langle \Gamma^2 \rangle - \langle \Gamma \rangle^2 / \langle \Gamma \rangle^2$), which is a measure of the width of the distribution of the decay rate. The measured diffusion coefficients were represented in terms of apparent radii by means of Stokes law.

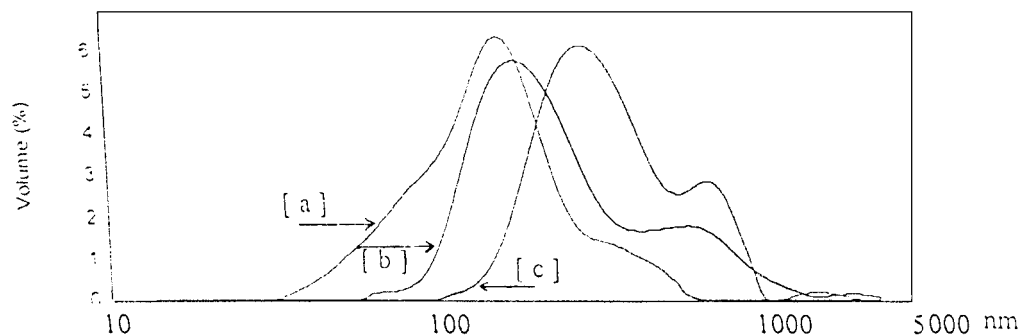


Figure 2 Particle size distribution of MMA-HEMA copolymer nanoparticles in the range of 80–90% conversions: (a) 90/10, (b) 80/20, and (c) 70/30 MMA/HEMA.

Scanning electron microscopy (SEM)

The effect of the variation in the HEMA content on the microstructure of the copolymer particles was studied with an ISI SX-40 scanning electron microscope (Wisconsin). The samples were coated with a gold film 2 μm thick before the analysis.

Thermal analysis

Differential scanning calorimetry (DSC) was performed with a Mettler-Toledo 822 instrument (Greifensee, Switzerland) at a heating rate of 5°C min^{-1} .

Drug release from nanoparticles

The drug release from nanoparticles was examined with the procedure reported by Basseur et al.¹⁰ The nanoparticles were dispersed into a 1% SLS solution, which according to U.S. pharmacopoeia is the dissolution medium of carbamazepine. The samples were withdrawn at regular time intervals and centrifuged. The supernatant was collected and analyzed at 285 nm for the drug content. The settled nanoparticles were redispersed into the dissolution medium.

TABLE I
Effects of the Monomer Ratio and Crosslinker Concentration on the Entrapment of Carbamazepine in the Copolymer Nanoparticles, Which Were Separated from the Dispersion with an (A) Excess of Methanol and (B) Cooling Below Kraft Temperature

Comonomer ratio (MMA/HEMA)	Entrapment A (%)	Entrapment B (%)	Effect of crosslinker concentration (%)		
			1%	2%	3%
90/10	61.2	69	72	73	73
80/20	63.2	74	76.4	78	79
70/30	65	78	80	84.4	85

RESULTS AND DISCUSSION

The variations in the HEMA concentration showed significant changes in the microstructure of the copolymer, from a more discrete structure at 90/10 MMA/HEMA to a networklike structure at 70/30 MMA/HEMA, with the yield above 90% in all the cases (Fig. 1). An increase in HEMA above 30% led to phase separation during polymerization. Schmuhl et al.¹¹ found similar variations in the copolymer microstructure for an MMA-HEMA/SLS/water microemulsion by changing the water content of the precursor microemulsions. The variation in the microstructure is important in this context because it affects both the drug entrapment and subsequently its release from the polymeric matrix. The highest entrapment was observed for the 70/30 MMA/HEMA system. This was a direct result of the difference in the monomer partitioning of MMA and HEMA in the different phases involved in the particle formation and the subsequent stabilization of the particles by the available surfactant. MMA, being less soluble in water than HEMA, partitions mainly in the micelles, whereas HEMA partitions primarily in the aqueous phase. Initiation with a water-soluble redox pair generates free radicals in the aqueous phase, to which monomer units dissolved in water are added, and polymer chains grow up to a critical length until they become surface-active. At this point, the probability of these surface-active free radicals entering the micelles is very high because of their higher residence time at the micelle-water interface, and this results in micellar nucleation. The further addition of monomer units beyond the critical chain length results in their precipitation in the aqueous phase; this is better known as homogeneous nucleation. The extensive work carried out by Gilbert¹² supports particle formation through such a mechanism for polar monomers, especially at a lower surfactant concentration. In addition, our earlier work on the emulsion polymerization of ethyl acrylate¹³ and its copolymerization with MMA¹⁴ showed that monomer

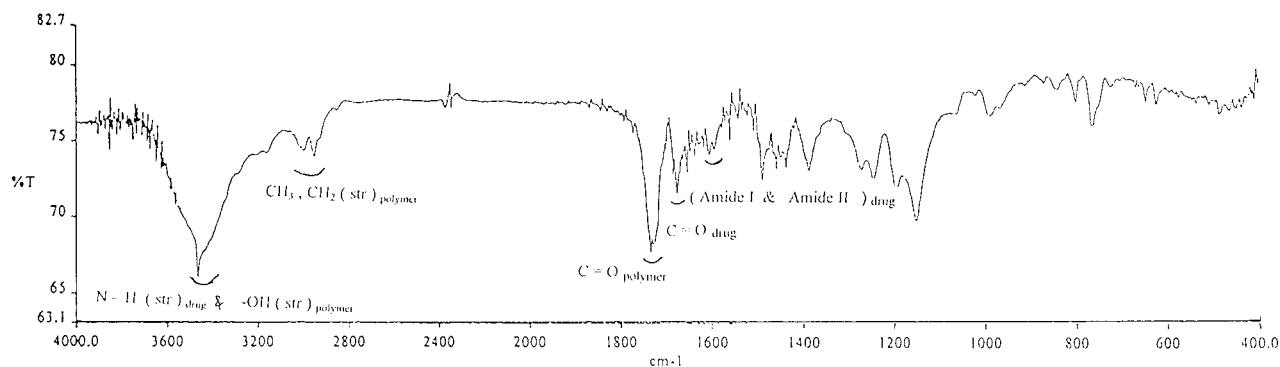


Figure 3 IR spectrum of the MMA-HEMA copolymer containing entrapped carbamazepine.

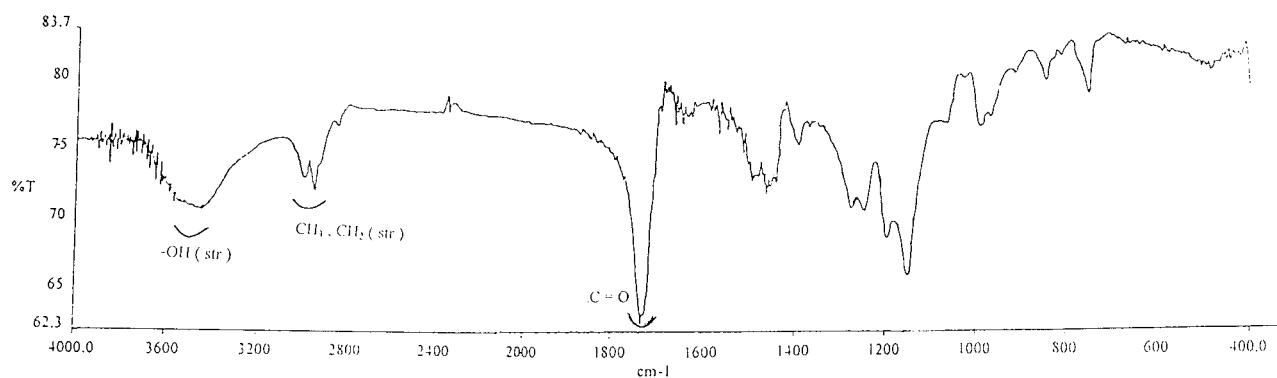


Figure 4 IR spectrum of the MMA-HEMA copolymer.

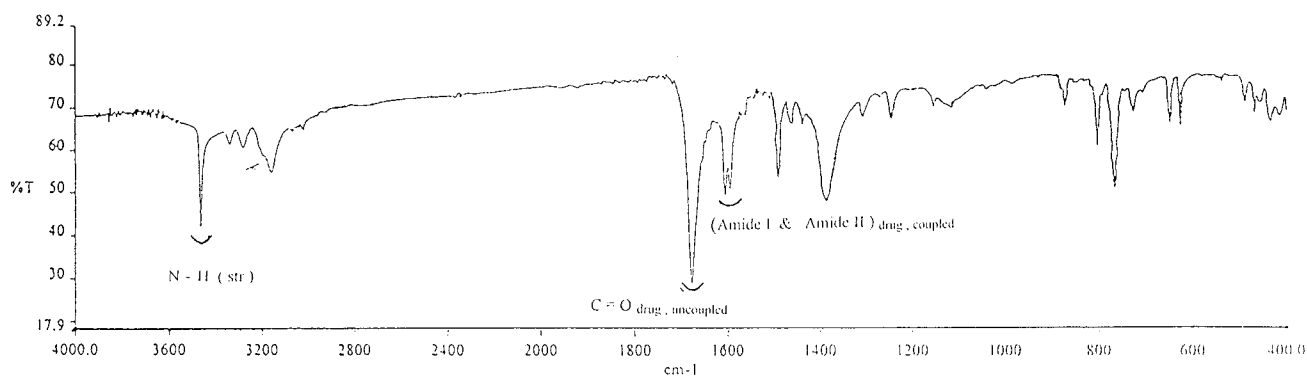


Figure 5 IR spectrum of carbamazepine.

partitioning leading to homogeneous nucleation strongly influenced the particle formation process and the final sizes of the polymer particles obtained. The critical chain length before precipitation depends on the hydrophobicity of the monomer units. The critical chain length for styrene has been reported¹² to be 2–3, whereas for MMA it is 4–5. In this case, the addition of water-soluble HEMA to MMA requires the addition of more monomer units than styrene or MMA before they actually precipitate to form a premature particle. The particles initially generated by homogeneous nucleation are colloiddally unstable and are prone to coagulation until they attain an optimum curvature of

the electrical double layer required for colloidal stability. This has been called the coagulative nucleation mechanism and is considered a subset of homogeneous nucleation.¹⁵ In this case, a very broad particle size distribution indicates particle formation involving more than one phase (Fig. 2). Furthermore, their bimodal nature is suggestive of polymerization, mainly through homogeneous-coagulative and micellar nucleation. With an increase in the HEMA concentration, the particle formation is dominated by homogeneous-coagulative nucleation, and the subsequent growth of these particles leads to increased coagulation and shows a shift toward a higher particle size distribu-

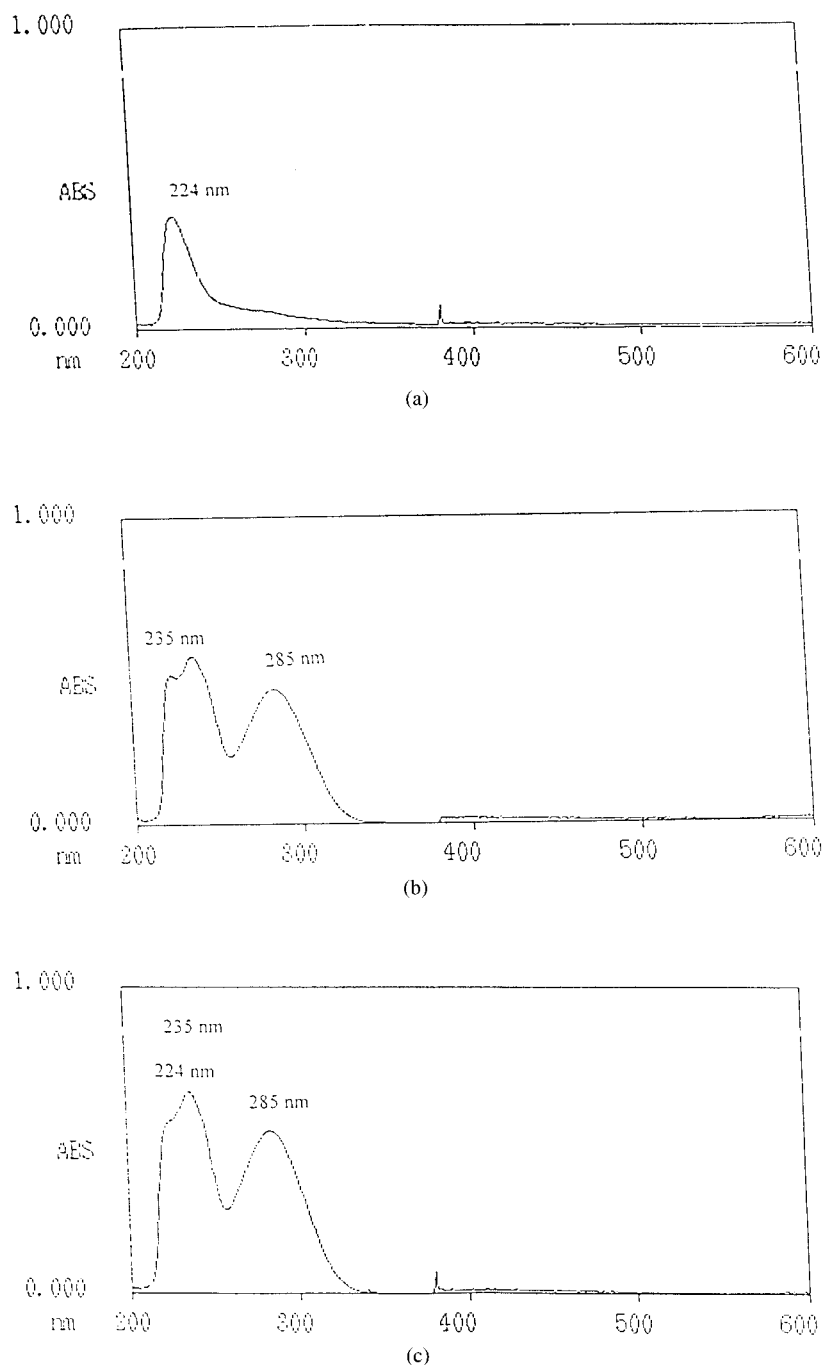


Figure 6 UV spectra of (a) the 70/30 MMA-HEMA copolymer, (b) the drug, and (c) the copolymer containing the drug.

tion. The volume-average diameters for 90/10, 80/20, and 70/30 were found to be 370, 435, and 655 nm, respectively. SEM also shows particle coagulation with an increase in the HEMA concentration [Fig. 1(c)]. Moreover, in the presence of micelles, HEMA partitions between the aqueous phase and the micelle-water interface. The cosurfactant effect of HEMA has been reported by a number of authors.^{11,16} Polymerization in an aqueous phase will drive the HEMA molecules from the interface to the aqueous phase to

maintain its saturation concentration in water. Because polymerization takes place in both the aqueous phase and micelles, this leads to a greater connectivity in the polymeric matrix with an increase in the HEMA concentration (Fig. 1).

When the HEMA concentration exceeds 30%, the surfactant concentration becomes insufficient to prevent heterocoagulation of the polymer particles generated through a coagulative nucleation mechanism, and this results in phase separation. The coagulative

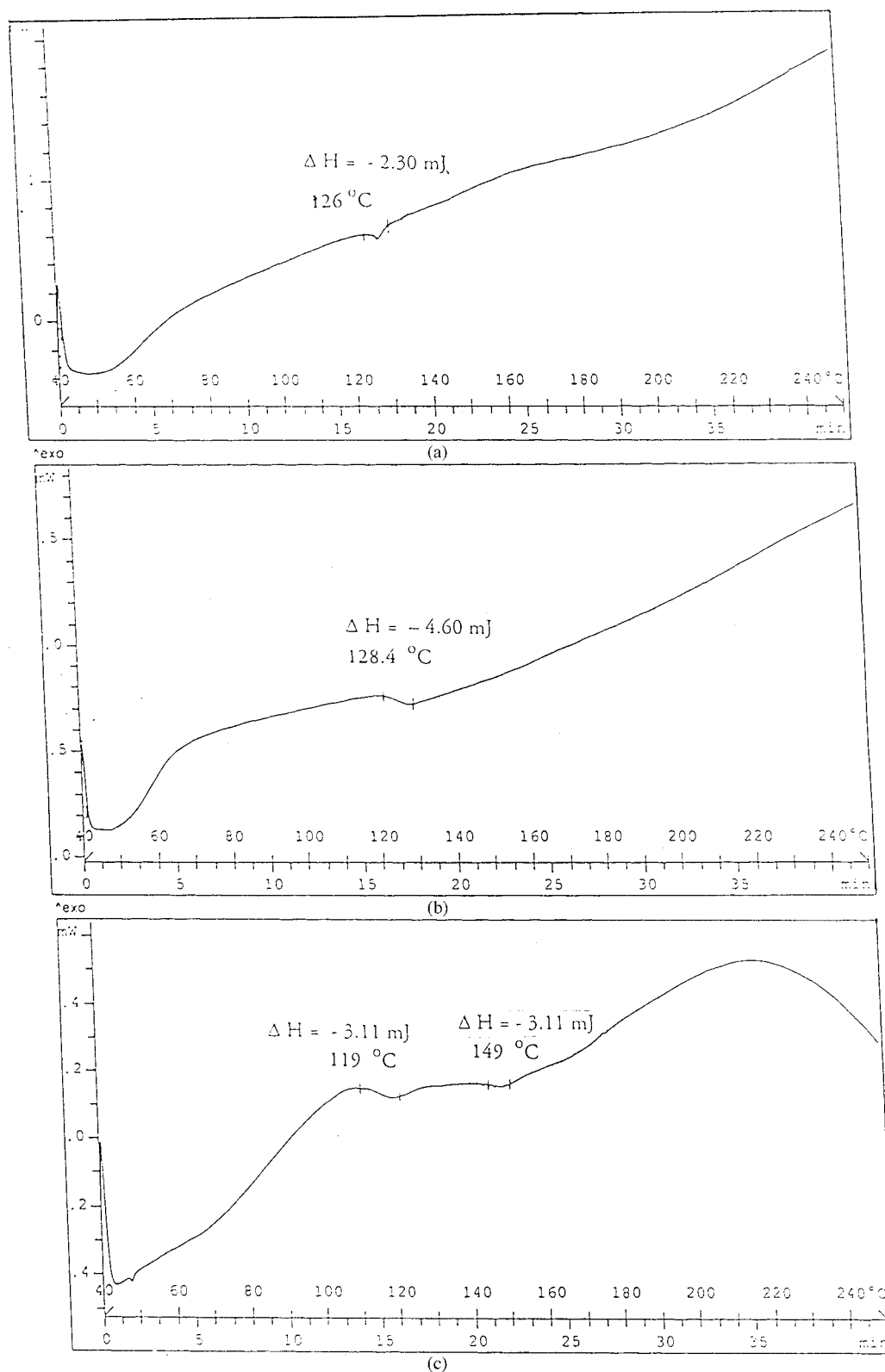


Figure 7 DSC thermograms of the MMA-HEMA copolymers with comonomer ratios of (a) 90/10, (b) 80/20, and (c) 70/30.

nucleation mechanism¹⁵ assumes heterocoagulation to be a kinetically faster process than the adsorption of the stabilizer. The previous observation indicates that

the entrapment efficiency of a drug should increase with an increase in the networking of the polymer matrix. Therefore, the effect of the crosslinker concen-

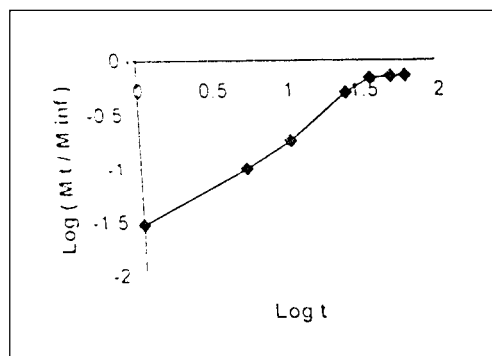
tration was also studied. The crosslinker EGDMA was used at 1, 2, and 3% concentrations (based on the monomer), and the drug entrapment efficiency showed a corresponding increase with increasing crosslinking (Table I).

The separation of the nanoparticles from a stable dispersion with methanol (method A) resulted in the leaching of the drug from the nanoparticles because of its solubility in methanol; this caused the entrapment efficiency to decrease. Alternatively, repeated freezing and thawing below and above the kraft temperature followed by freeze drying of the nanoparticles (method B) for isolation improved the entrapment efficiency (Table I).

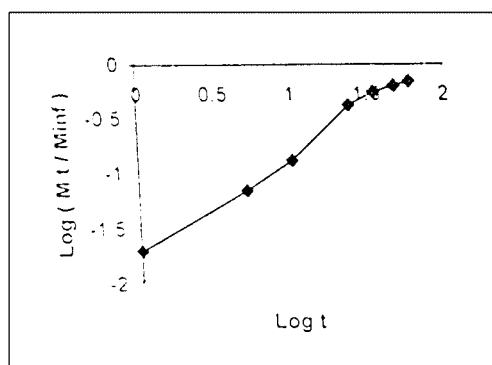
IR analysis further confirmed drug entrapment in the polymeric matrix (Fig. 3). IR spectra show C=O (stretching) due to both MMA and HEMA units in the copolymer at 1734 cm^{-1} , whereas C=O (stretching) due to amide groups from carbamazepine appears at 1677 cm^{-1} , which is free from the coupled vibration because of the involvement of the tertiary nitrogen of the ring. The C=O (stretching) and N—H (deformation) coupled vibrations, giving rise to the characteristic amide I and II bands, can be seen at 1605 and 1595 cm^{-1} , respectively. A broad band around 3650 cm^{-1} arises because of —OH (stretching) from HEMA. The absorbance at 3466 cm^{-1} is due to N—H (stretching) for carbamazepine. Bands due to CH_3 and CH_2 (stretching) vibrations appear around 2953 cm^{-1} . Band assignments were made with respect to the reference spectra of the MMA-HEMA copolymer (Fig. 4) and drug (Fig. 5), respectively. The UV spectra of the 70/30 MMA-HEMA copolymer, the drug, and the drug-containing copolymer are given in Figure 6. The wavelengths of the maximum absorbance of the drug were observed to be 235 and 285 nm [Fig. 6(b)], although the copolymer showed maximum absorbance at 224 nm [Fig. 6(a)].

A DSC scan [Fig. 7(a,b)] shows glass-transition temperatures (T_g 's) of 126 and 128.4°C for 90/10 and 80/20 MMA/HEMA, respectively. For 70/30 MMA/HEMA [Fig. 7(c)], the appearance of two T_g 's around 119 and 149°C is suggestive of two different compositions of the polymer chains due to the involvement of two phases in particle formation. The appearance of two T_g 's due to the compositional heterogeneity of the copolymers was also reported by us in the emulsion copolymerization of a partially water-soluble monomer, ethyl acrylate, and MMA, with a wide difference in the T_g values of the homopolymers.

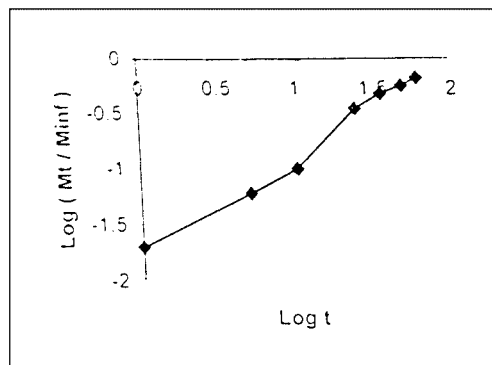
The release of carbamazepine from the nanoparticles was studied through the suspension of the dispersion in a 1% SLS solution. Drug-release studies of the nanoparticles were carried out with three different ratios of MMA and HEMA. The nanoparticles with 90/10 MMA/HEMA showed greater drug release than the nanoparticles with 80/20 and 70/30 MMA/



(a)



(b)



(c)

Figure 8 Drug release from copolymer nanoparticles containing (a) 90/10, (b) 80/20, and (c) 70/30 MMA/HEMA.

HEMA (Fig. 7). The reason for slower drug release in 70/30 MMA/HEMA may be the greater degree of coagulation, as shown by Figure 1(c), which leads to a reduced effective surface area. Generally, more drug release can be expected from a copolymer system with an increased HEMA concentration because of its higher solubility in water. On the contrary, faster drug release was found with the 90/10 MMA/HEMA system. This was due to the more discrete nature of the

particles, which resulted in a larger effective surface area, as shown in Figure 1(a). The release profiles of $\log(M_t/M_\alpha)$, the log of the fractional amount released, versus $\log t$ of carbamazepine from the poly(MMA-co-HEMA) nanoparticles show a prolonged time up to 70% in 48 h. The kinetics of the drug release were studied by the general equation of Sinclair and Peppas:¹⁷

$$M_t/M_\alpha = kt^n \quad (1)$$

$$\log(M_t/M_\alpha) = \log k + n \log t \quad (2)$$

where k is the diffusional constant and n is the diffusional exponent. This shows that the kinetics of release approach zero order for 80/20 and 70/30 MMA/HEMA [Fig. 8(b,c)] and a biphasic release for the 90/10 MMA/HEMA system, reaching saturation after 35 h [Fig. 8(a)].

CONCLUSIONS

The copolymer microstructure has been found to be sensitive to the presence of the polymerizable cosurfactant HEMA. An increase in the HEMA concentration leads to a shift in particle formation, mainly through a coagulative nucleation mechanism, leading to a greater connectivity of the polymeric matrix, as shown by SEM and also indicated by a broadening particle size distribution. This results in an increase in drug entrapment and a slower release of the drug

from copolymer nanoparticles. Also, the release kinetics approach zero order with an increase in the HEMA concentration.

References

1. Kreuter, J. In *Microcapsules and Nanoparticles in Medicine and Pharmacy*; Donbrow, M., Ed.; CRC: Boca Raton, FL, 1992.
2. Youssef, M.; Fattal, E.; Alonso, M. J.; Roblot-Treupel, L.; Sauzieres, J.; Tanerede, C.; Omnes, C.; Couvreur, A.; Andremont, A. *Antimicrob Agents Chemother* 1988, 32, 1204.
3. Kreuter, J. *Colloidal Drug Delivery Systems*; Marcel Dekker: New York, 1994.
4. Fitch, R. M.; Prenosil, M. B.; Sprick, K. J. *J Polym Sci Part C: Polym Symp* 1969, 27, 95.
5. Kreuter, J. *J Polym Sci Polym Lett Ed* 1982, 20, 543.
6. Couvreur, P.; Kante, B.; Roland, M.; Guiot, P.; Baudhuin, P.; Speiser, P. *J Pharm Pharmacol* 1979, 31, 331.
7. Kreuter, J.; Liehl, E.; Berg, U.; Soliva, M.; Speiser, P. *Vaccine* 1998, 6, 253.
8. Rembaum, A.; Yen, S. P. S.; Molday, R. S. *J Macromol Sci Chem* 1979, 13, 603.
9. Sivakumar, M.; Rao, K. P. *J Appl Polym Sci* 2002, 83, 3045.
10. Brasseur, N.; Brault, D.; Couvreur, P. *Int J Pharm* 1991, 70, 129.
11. Schmuhl, N.; Davis, E.; Cheung, H. M. M. *Langmuir* 1998, 14, 757.
12. Gilbert, R. G. *Emulsion Polymerization: A Mechanistic Approach*; Academic: London, 1995.
13. Bhawal, S.; Pokhriyal, N. K.; Devi, S. *Eur Polym J* 2002, 38, 735.
14. Bhawal, S.; Dhoble, D.; Devi, S. *J Appl Polym Sci* 2003, 90, 2593.
15. Feeney, P. J.; Napper, D. H.; Gilbert, R. G. *Macromolecules* 1984, 17, 2520.
16. Candau, F. In *Structures: Microemulsions and Liquid Crystals*; Nokaly, E. L., Ed.; ACS Symposium Series 384; American Chemical Society: Washington, DC, 1989.
17. Sinclair, G. W.; Peppas, N. A. *J Membr Sci* 1984, 17, 329.